

Gene Expression Differences in Normal Esophageal Mucosa Associated with Regression and Progression of Mild and Moderate Squamous Dysplasia in a High-Risk Chinese Population

Nina Joshi,¹ Laura Lee Johnson,³ Wen-Qiang Wei,⁶ Christian C. Abnet,² Zhi-Wei Dong,⁶ Philip R. Taylor,⁴ Paul J. Limburg,⁷ Sanford M. Dawsey,² Ernest T. Hawk,⁵ You-Lin Qiao,⁶ and Ilan R. Kirsch¹

¹Genetics Branch, Center for Cancer Research and ²Nutritional Epidemiology Branch, Division of Cancer Epidemiology and Genetics, National Cancer Institute (NCI); ³Office of Clinical and Regulatory Affairs, National Center for Complementary and Alternative Medicine and ⁴Genetic Epidemiology Branch, Division of Cancer Epidemiology and Genetics, NIH; ⁵Office of Centers, Training, and Resources, NCI, NIH, Bethesda, Maryland; ⁶Cancer Institute, Chinese Academy of Medical Sciences, Beijing, China; and ⁷Mayo Clinic College of Medicine, Rochester, Minnesota

Abstract

A randomized, double-blinded, placebo-controlled 2×2 factorial chemoprevention trial was conducted in Linxian, China to assess the effects of selenomethionine and celecoxib on the natural history of esophageal squamous dysplasia. Results from this study indicated that asymptomatic adults with mild dysplasia were more likely to show an improvement when treated with selenomethionine compared with placebo ($P = 0.02$). Prompted by this finding, we examined the molecular profiles associated with regression and progression of dysplastic lesions in normal mucosa from 29 individuals, a subset of the Linxian cohort, using the Affymetrix U133A chip. Twenty differentially expressed genes were associated with regression and 129 were associated with progression when we compared the change in gene expression over time. Genes associated with immune response ($n = 15$), cell cycle ($n = 15$), metabolism ($n = 15$), calcium transport or calcium ion activity ($n = 10$), regulation of transcription ($n = 9$), signal transduction ($n = 7$), cytoskeleton and microtubules ($n = 5$), nucleotide processing and biosynthesis ($n = 4$), G-coupled signaling ($n = 4$), and apoptosis ($n = 3$) were present in the list of 149 genes. Using the Expression Analysis Systematic Explorer pathway analysis program, only the immune response pathway was significantly overrepresented among these 149 genes. Individuals whose lesions regressed seemed to have higher expression of genes associated with immune stimulation, such as antigen presentation, survival of T cells, and T-cell activation (*HLA-DRA*, *HLA-DPA1*, *HLA-DBQ1*, *CD58*, and *FCER1A*). In contrast, individuals whose lesions progressed had higher expression of genes involved in immune suppression and inflammation (*CNR2*, *NFATC4*, *NFRKB*, *MBP*, *INHBB*, *CMKLR1*, *CRP*, *ORMS*, *SERPINA7*, and

SERPINA1). These data suggest that local and systemic immune responses may influence the natural history of esophageal squamous dysplasia. (Cancer Res 2006; 66(13): 6851-60)

Introduction

Esophageal cancer is the sixth most common cause of cancer death worldwide, with >400,000 new cases diagnosed each year (1). Because symptoms typically remain absent until late in the course of disease, most cancers are detected at an advanced stage when prognosis is poor. The overall 5-year survival rate for esophageal cancer in the United States is 13% (2), which is similar to the observed rates in China and other global regions. To reduce the health burden of esophageal cancers, new intervention strategies are being examined, including chemoprevention, for select high-risk populations. The close association between histologic grading of squamous dysplasia and risk of future esophageal squamous cell carcinoma (ESCC) suggests that a shift in grade of dysplasia corresponds to a real change in cancer risk. In Linxian China, a region with some of the highest incidence and mortality rates of ESCC in the world, a recent study showed that the relative risks for developing ESCC over 13 years of follow-up were 2.9, 9.8, and 28.3 for individuals with mild, moderate, or severe dysplasia, respectively, compared with persons without histologic evidence of dysplasia or cancer (3). In a large prospective study conducted earlier in Linxian, higher serum selenium was associated with a significantly reduced risk of developing ESCC (4). Epidemiologic studies have also associated nonsteroidal anti-inflammatory drug use with reduced risk of esophageal cancer (5, 6). Based on these results, a randomized, double-blinded, placebo-controlled 2×2 factorial chemoprevention trial was conducted in Linxian to assess the short-term effects of selenomethionine and celecoxib (a selective inhibitor of cyclooxygenase-2) on the progression of esophageal squamous dysplasia (7). Asymptomatic adults with histologically confirmed dysplasia, graded as either mild or moderate according to established criteria (8), at baseline were enrolled and randomly assigned to one of four intervention groups: selenomethionine (200 μ g daily), celecoxib (200 mg twice daily), both selenomethionine and celecoxib, or placebo. The response to the intervention agents was assessed by the change in each patient's worst grade of squamous dysplasia between baseline and 10 months, and study participants were categorized as experiencing regression, stable disease, or progression. The results of this

Note: Current address for N. Joshi: UES, Inc., 4401 Dayton-Xenia Road, Dayton, OH 45432-1894; I.R. Kirsch: Amgen, 1201 Amgen Court West, AW1-J 4144, Seattle, WA 98119-3105.

Requests for reprints: Philip R. Taylor, Division of Cancer Epidemiology and Genetics, National Cancer Institute, NIH, EPS, 6120 Executive Boulevard, Room 7006, Bethesda, MD 20892-7236. Phone: 301-594-2932; Fax: 301-402-4489; E-mail: ptaylor@mail.nih.gov.

©2006 American Association for Cancer Research.
doi:10.1158/0008-5472.CAN-06-0662

study showed that selenomethionine treatment increased regression and decreased progression among patients who began the trial with mild dysplasia ($P = 0.02$) but not among those who began with moderate dysplasia ($P = 1.00$). Celecoxib had no apparent effect on dysplasia grade ($P = 0.78$; ref. 7).

The precise molecular targets associated with regression and progression of squamous dysplastic lesions in the esophagus have not been identified. The present study aimed to address this knowledge gap. We used microarray analysis to assess changes in gene expression before and after treatment in histopathologically confirmed normal mucosa taken from 29 individuals, a subset of the 117 subjects in the selenomethionine and placebo arms of the original Linxian chemoprevention trial cohort. This subset included 11 individuals whose dysplasia regressed, 13 who were stable, and 5 whose dysplasia progressed.

Materials and Methods

Intervention procedures and sample collections. The randomized, double-blinded, placebo-controlled chemoprevention trial, which was the basis of this analysis, is described elsewhere (7). In short, potential subjects were recruited from eight villages in the northern part of Linxian beginning in April 1999. Residents who agreed to participate were submitted to an initial screening evaluation. Subjects underwent endoscopy with Lugol's iodine staining and biopsies, and those who had at least one grossly visible lesion diagnosed histologically as mild or moderate squamous dysplasia were potentially eligible for the chemoprevention trial (7). Subjects were stratified by gender and randomly assigned using a variable block approach with an allocation ratio of 1:1:1:1 for selenomethionine and celecoxib (group 1), celecoxib only (group 2), selenomethionine only (group 3), and placebo (group 4). Doses for the active arms were 200 μ g selenomethionine once daily and 200 mg celecoxib twice daily for a total of 10 months. Compliance was assessed by direct observation of all morning doses, by pill counts, and by serum selenium measurements.

Baseline and end-of-trial esophagogastrroduodenoscopy exams were done using Pentax videoendoscopy equipment (Pentax Precision Instrument Corp., Orangeburg, NY). Following initial inspection, the esophageal mucosa was sprayed with 1.2% Lugol's iodine solution, after which dysplastic lesions appear unstained relative to the surrounding normal mucosa (9). All unstained lesions ≥ 5 mm in diameter were biopsied. In addition, two adjacent biopsy samples were obtained from endoscopically normal mucosa located at least 10 mm away from any grossly visible lesion. One of these latter biopsies was snap frozen in liquid nitrogen, and the other was fixed and processed along with the lesion biopsies. The fixed biopsy samples were immediately placed in 10% neutral-buffered formalin, embedded in paraffin, sectioned in 5- μ m thicknesses, and stained with H&E. The biopsy slides from the baseline and end-of-trial endoscopy exams for each patient were paired and reviewed together, with the dates of the exams masked. The slides were independently reviewed in a blinded fashion by two gastrointestinal pathologists who were unaware of the intervention group assignments. Cases with discrepant results were adjudicated in a blinded fashion by a third gastrointestinal pathologist. The study was approved by the Institutional Review Boards of the Cancer Institute, Chinese Academy of Medical Sciences (Beijing, China) and the U.S. National Cancer Institute (Bethesda, MD).

Sample selection for expression analysis. Baseline and end-of-trial frozen biopsies from endoscopically normal mucosa were available from 66 individuals from the selenomethionine and placebo arms of the chemoprevention trial. The adjacent fixed biopsies were histologically normal at both time points in 29 individuals, and the frozen biopsies from these cases were used for the microarray analyses.

Microarray experiments. Total RNA was isolated from the snap-frozen biopsies using the Qiagen (Valencia, CA) RNeasy Mini kit and a Micro-H Omni (Marietta, GA) homogenizer. RNA quality was examined using the RNA 6000 Nano assay on the Agilent (Palo Alto, CA) 2100 Bioanalyzer. The

Affymetrix (Santa Clara, CA) small sample labeling protocol vII was used as specified by the manufacturer (10). In short, two cycles of linear amplification were done. cDNA was first synthesized from 1 μ g total RNA using a first-strand and a second-strand protocol, with the T7-oligo(dT) promoter primer used for the first-strand synthesis. The double-stranded cDNA was purified by ethanol precipitation, amplified with the Ambion (Austin, TX) MEGA-script T7 kit, and then purified again using the RNeasy kit. cRNA (2 μ g), quantified by spectrophotometer, was then used to resynthesize cDNA with a random primer for the first-strand synthesis and the T7-oligo(dT) promoter primer for the second-strand synthesis. The cDNA was purified by ethanol precipitation and biotin labeled with the ENZO BioArray High Yield RNA Transcript labeling kit purchased from Affymetrix. The labeled cRNA was then purified using the RNeasy columns. The cRNA concentration was measured by a spectrophotometer and fragmented.

The GeneChip Human Genome U133A platform was used, which consists of 22,000 oligonucleotide probe sets representing 18,400 transcripts and variants, including 14,500 known genes. The GeneChips were prehybridized using 1 \times hybridization buffer [100 mmol/L MES, 1 mol/L Na⁺, 20 mmol/L EDTA, 0.01% Tween 20 (final concentration)] at 65°C, with 60 rpm rotation for 10 minutes. The prehybridization solution was removed and replaced with denatured hybridization solution containing 0.06 μ g/ μ L fragmented cRNA (15 μ g in total), 50 pmol/L control oligonucleotide B2, 1.5, 5, 25, and 100 pmol/L, respectively, of 20 \times eukaryotic hybridization controls (*bioB*, *bioC*, *bioD*, and *cre*), and 0.1 mg/mL herring sperm DNA. The hybridizations were done in an oven at 65°C, rotating at 60 rpm for 16 hours. Protocol EukGe_WS2v5_450 was used to wash and stain the GeneChips on Affymetrix Fluidics Station 450. The arrays were washed with a series of nonstringent (wash A: 6 \times saline-sodium phosphate-EDTA, 0.01% Tween 20) and stringent (wash B: 100 mmol/L MES, 0.1 mol/L Na⁺, 0.01% Tween 20) wash buffers and stained with streptavidin phycoerythrin [1 \times MES stain buffer, 2 mg/mL acetylated bovine serum albumin (BSA), 10 μ g/mL streptavidin phycoerythrin]. The signal was then amplified with an antibody solution (1 \times MES stain buffer, 2 mg/mL acetylated BSA, 0.1 mg/mL normal goat IgG, 3 μ g/mL biotinylated antibody) and stained a second time with streptavidin phycoerythrin.

Microarray image acquisition and data analysis. The probe arrays were scanned in an Affymetrix GeneChip Operating Software Scanner 3500 equipped with an argon-ion laser at the excitation wavelength of 488 nm. Signal intensities were calculated from the cellular intensity files (.cel) files, generated by the GeneChip Operating System, using justRMA, a library of Bioconductor (version 1.9) supported by R (version 1.8.1). We also used database for annotation, visualization, and integrated discovery (DAVID) and NetAffx, genomic databases, for gene annotation (11).

Statistical analysis. We analyzed mRNA expression levels in normal mucosa samples from individuals categorized as regressors, stable, or progressors based on the change in their worst histologic lesions over a period of 10 months. For subjects whose most advanced histologic diagnosis at baseline was mild dysplasia, regression was defined as no evidence of dysplasia, whereas progression was defined as moderate dysplasia, severe dysplasia, or invasive carcinoma. For subjects whose most advanced histologic diagnosis at baseline was moderate dysplasia, regression was defined as no evidence of dysplasia or mild dysplasia, whereas progression was defined as severe dysplasia or invasive carcinoma.

We examined whether the change in gene expression between T_0 and T_{10} was associated with regression, stability, or progression of esophageal squamous dysplasia. A standard t test, often associated with microarray analysis, could not be used to analyze the data generated from this study because there are three different response groups instead of the usual two. These three ordinal categories dictated the use of ordinal regression (12). The selenomethionine treatment effects were adjusted for by placing this covariate into the ordinal regression model. The direction of the β coefficient for gene expression change indicates whether the change was associated with regression (negative) or progression (positive). The coefficients and the corresponding P s generated from this model assumed a linear trend in relative gene expression. For example, for a gene with relatively increased expression in individuals whose lesions regressed, there is intermediate expression in individuals whose lesions were stable and

lower expression in individuals whose lesions progressed. Conversely, genes associated with progression will also maintain this linear relationship in reverse (greater expression in individuals whose lesions progressed, intermediate in stable individuals, and lower expression in individuals whose lesions regressed).

We searched for genes associated with regression, stable, and progression using two different definitions of statistical significance. For the first definition, we used only a P cutoff of $P < 0.001$ (Tables 2 and 3). Our second definition was more stringent and required, in addition to a $P < 0.001$, a magnitude component (i.e., that the range of gene expression be at least 2-fold; Fig. 1).

Pathway analysis of microarray data. The genes that were statistically significantly different in the ordinal regression analysis were examined using the Gene Ontology biological process database and the Expression Analysis Systematic Explorer (EASE version 2.0) program (13). The Gene Ontology database categorizes genes in proven or probable functional groups. EASE is a customized, stand-alone software application with statistical functions for discovering biological themes within gene lists. It assigns genes of interest into functional categories based on the Gene

Ontology database and uses the Fisher's exact test statistic to determine the probability of observing the number of genes within a list of interest versus the number of genes in each category on the array. Gene symbols retrieved from December 20, 2005 Affymetrix update were used for this analysis.

Results

The 29 individuals used for this analysis had similar characteristics to the final analytic cohort ($n = 117$) included in the parent chemoprevention trial (Table 1). There were no differences between these two populations in age, sex, body mass index, tobacco use, alcohol consumption, baseline serum selenium level, number of biopsy samples, proportion of individuals with mild or moderate dysplasia at baseline, or proportion of individuals assigned to the selenomethionine and the placebo groups. Eleven of the individuals used for this analysis were classified as regressors, 13 were stable, and 5 were progressors.

Figure 1. Forty-eight of the 149 genes associated with regression or progression also had a range of expression that was at least 2-fold. The ordinal regression model defined regress as (-1), stable as (0), and progress as (1). Seventeen genes had $\beta < 0$ and were associated with regression; 31 genes with $\beta > 0$ were associated with progression.

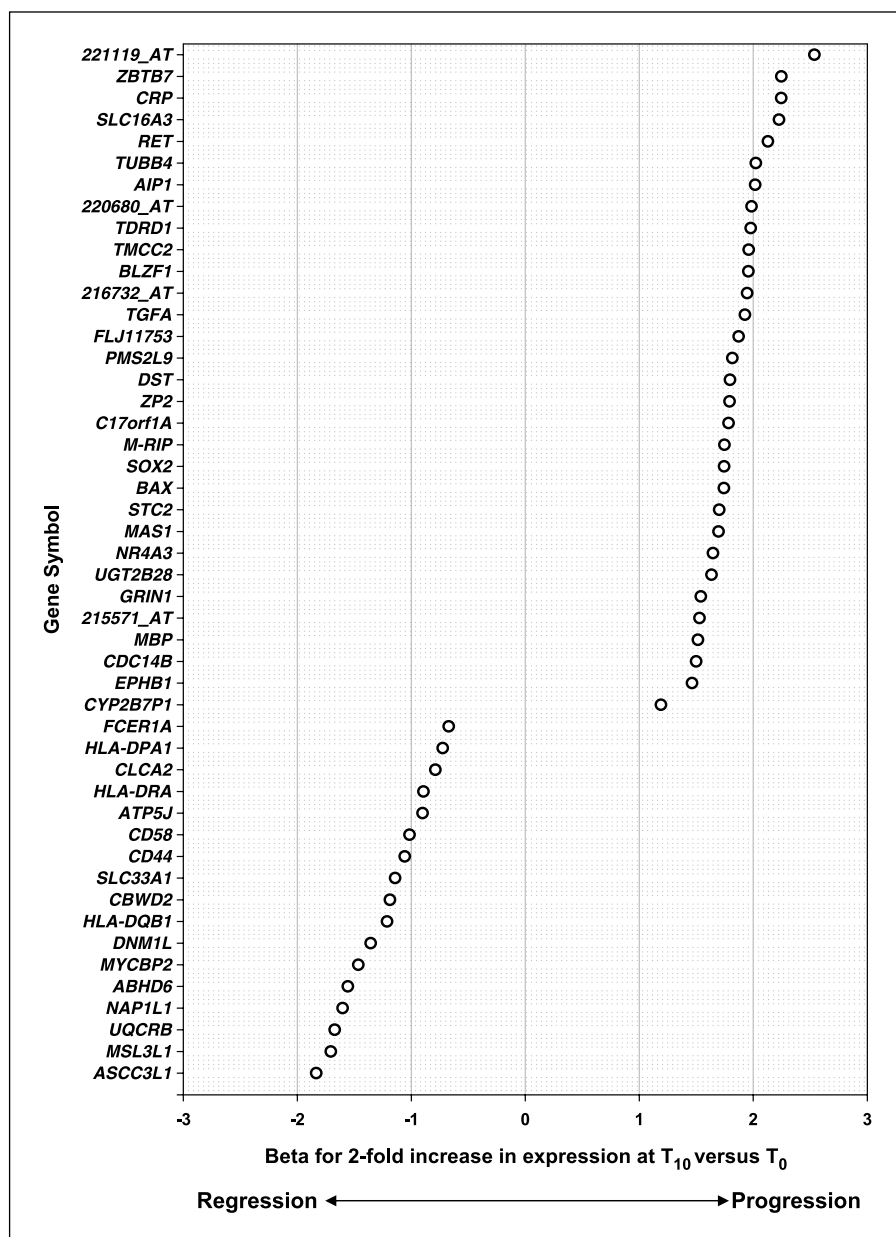


Table 1. Baseline characteristics for the selenomethionine-only and placebo-only groups in the full trial analytic cohort ($n = 117$) and in the Affymetrix substudy ($n = 29$)

| Study agent | Full trial analytic cohort ($n = 117$) | | Affymetrix substudy ($n = 29$) | |
|--|--|------------------------------|---------------------------------------|------------------------------|
| | Selenomethionine only ($n = 59$) | Placebo only ($n = 58$) | Selenomethionine only ($n = 13$) | Placebo only ($n = 16$) |
| Age, y [mean (SD)] | 48 (5.6) | 48 (6.3) | 48 (5.0) | 48 (7.0) |
| Gender (% female) | 53 | 57 | 62 | 63 |
| Body mass index, kg/m ² [mean (SD)] | 22.4 (2.6) | 22.7 (2.8) | 22.4 (1.8) | 23.2 (3.2) |
| Tobacco use (% ever) | 29 | 26 | 31 | 13 |
| Alcohol use (% yes) | 53 | 36 | 46 | 38 |
| Serum selenium, µg/L [median (interquartile range)] | 85 (75-98) | 79 (68-97) | 84 (75-102) | 75 (68-95) |
| No. biopsy samples taken [mean (range)] | 6.1 (3-11) | 5.9 (3-12) | 6.1 (4-9) | 6.0 (4-10) |
| Moderate dysplasia (%) | 49 | 52 | 38 | 44 |
| Mild dysplasia (%) | 51 | 48 | 62 | 56 |

Using a cutpoint of $P < 0.001$, we identified 149 genes expressed in the normal esophageal mucosa that were associated with regression or progression of their worst squamous diagnosis from baseline to the end of the intervention when analyzing paired data (the difference in expression within the normal mucosa at baseline versus normal mucosa obtained at the end of intervention). Higher expression of 20 genes (Table 2) was associated with regression, whereas higher expression of 129 genes (Table 3) was associated with progression. For 48 of these 149 genes, the range of gene expression was at least 2-fold (Fig. 1), including 17 genes associated with regression and 31 associated with progression.

We analyzed these data on the log₂ scale, so a 1-unit increase in the gene expression covariate was equivalent to a 2-fold increase in gene expression from baseline to 10 months. Additionally, the interpretation of coefficients in this model is slightly different than in most t test models. Although one can discuss underexpression and overexpression, for research purposes we preferred to think about overexpression in a gene trending toward regression or progression of esophageal squamous dysplasia. Figure 1 depicts the β coefficients from the analyses in a continuum along the X axis, where zero means the three groups of individuals (those who had regression, stability in worst diagnosis, or progression) had similar

Table 2. Twenty genes whose increased expression was associated with regression of dysplasia

| Gene name or Affymetrix ID | Gene symbol | UniGene ID | β^* | Range of gene expression | P |
|--|------------------|------------|-----------|--------------------------|----------|
| Ribosomal protein S24 | <i>RPS24</i> | Hs.356794 | -2.093 | 2.00 | 0.000732 |
| Retinol dehydrogenase 11 | <i>RDH11</i> | Hs.226007 | -2.062 | 1.95 | 0.000096 |
| Activating signal cointegrator 1 complex subunit 3-like 1 | <i>ASCC3L1</i> | Hs.246112 | -1.834 | 2.27 | 0.000919 |
| Kinesin family member 5B | <i>KIF5B</i> | Hs.327736 | -1.758 | 1.95 | 0.000566 |
| Male-specific lethal 3-like 1 | <i>MSL3L1</i> | Hs.307924 | -1.707 | 2.28 | 0.000698 |
| Ubiquinol-cytochrome <i>c</i> reductase binding protein | <i>UQCRB</i> | Hs.131255 | -1.672 | 2.24 | 0.000310 |
| Nucleosome assembly protein 1-like 1 | <i>NAP1L1</i> | Hs.524599 | -1.602 | 2.48 | 0.000572 |
| Abhydrolase domain containing 6 | <i>ABHD6</i> | Hs.476454 | -1.557 | 2.16 | 0.000741 |
| MYC binding protein 2 | <i>MYCBP2</i> | Hs.151411 | -1.464 | 3.72 | 0.000026 |
| Dynamin 1-like | <i>DNM1L</i> | Hs.550499 | -1.356 | 2.69 | 0.000496 |
| MHC, class II, DQ β 1 | <i>HLA-DQB1</i> | Hs.409934 | -1.213 | 2.73 | 0.000410 |
| COBW domain containing 1/2/3 | <i>CBWD1/2/3</i> | Hs.355950 | -1.187 | 3.14 | 0.000132 |
| Solute carrier family 33 member 1 | <i>SLC33A1</i> | Hs.478031 | -1.142 | 3.61 | 0.000972 |
| CD44 antigen | <i>CD44</i> | Hs.502328 | -1.058 | 4.87 | 0.000160 |
| CD58 antigen, (lymphocyte function-associated antigen 3) | <i>CD58</i> | Hs.34341 | -1.016 | 2.94 | 0.000517 |
| ATP synthase, H ⁺ transporting, mitochondrial F0 complex, subunit F6 | <i>ATP5J</i> | Hs.246310 | -0.901 | 4.74 | 0.000416 |
| MHC, class II, DR α | <i>HLA-DRA</i> | Hs.520048 | -0.894 | 4.37 | 0.000049 |
| Chloride channel, calcium activated, family member 2 | <i>CLCA2</i> | Hs.241551 | -0.789 | 4.45 | 0.000972 |
| MHC, class II, DP α 1 | <i>HLA-DPA1</i> | Hs.347270 | -0.725 | 6.41 | 0.000873 |
| Fc fragment of IgE, high affinity I, receptor for; α polypeptide//Fc fragment of IgE, high affinity I, receptor for; α polypeptide | <i>FCERIA</i> | Hs.897 | -0.671 | 8.60 | 0.000152 |

* β s were generated from the ordinal regression model, which defined regress as (-1), stable as (0), and progress as (1). Twenty genes were associated with regression. The more negative the value, the greater the association with regression.

changes in gene expression over the 10-month period. The more negative a coefficient, the stronger a 2-fold increase in the gene expression over the 10-month period pulls toward the regression end of the continuum. The more positive a coefficient, the stronger a 2-fold increase in the gene expression over the 10-month period pulls toward the progression end of the continuum. These coefficients are similar to point estimates, but they are not fold changes. Every value is based on what occurs to esophageal dysplasia status given a 2-fold increase in the RNA expression of a particular gene from the beginning to the end of the intervention period.

Using the Gene Ontology database, we categorized the 149 differentially expressed genes into known or probable functional categories. The most common categories included immune response (15 genes: *FCER1A*, *CD58*, *HLA-DPA1*, *HLA-DRA*, *HLA-DQB1*, *CRP*, *ORMS*, *SERPINA7*, *SERPINA1*, *CNR2*, *NEATC4*, *NFRKB*, *MBP*, *INHBB*, and *CMKLR1*), cell cycle (15 genes: *RET*, *TGF- α* , *MET*, *CDC14B*, *CDC42*, *DLG3*, *EGR4*, *IL9*, *MAS1*, *NAPILI*, *CDC25C*, *SOCS1*, *APBB2*, *BLZF1*, and *NPPB*), metabolism (15 genes: *RDH11*, *AGPAT3*, *UGT2B28*, *GBA3*, *CHAT*, *HSD11B1*, *ATP12A*, *DCT*, *ABCA1*, *UQCRB*, *ATP5J*, *PPARA*, *PNLIPRP2*, *TXNRD2*, and *ABHD6*), calcium transport or calcium ion activity (10 genes: *THBS1*, *TACSTD2*, *CADPS*, *RAMP3*, *CLCA2*, *CDH9*, *GRIN1*, *TRPC4*, *STC2*, and *ZZEF1*), regulation of transcription (9 genes: *ZBTB7A*, *ZNF480*, *KIAA0194*, *GTF2A1*, *PRDM10*, *ZNF1A1*, *NR4A3*, *ZNF42*, and *MYCBP2*), signal transduction (7 genes: *PNOC*, *EPHBI*, *BRAP*, *SEMA4F*, *GP6*, *NPPB*, and *PHEX*), cytoskeleton and microtubules (5 genes: *KIF5B*, *RDX*, *TUBB5*, *DST*, and *ASTN*), nucleotide processing and biosynthesis (4 genes: *MTAP*, *SLC29A1*, *ADCY2*, and *UMPS*), G-coupled signaling (4 genes: *F2RL2*, *GRPR5*, *BAI3*, and *RASL113*), and apoptosis (3 genes: *CASP2*, *BAX*, and *CIDEA*).

We used the EASE software package to identify pathways overrepresented in the 149 differentially expressed genes. The 15 genes associated with the immune response pathway were greater than the expected number based on the total number of immune response genes on the microarray chip ($P < 0.01$). No other pathway was overrepresented in the 149 genes we found in our analysis. Further analysis of the immune response genes revealed that those associated with regression had functions consistent with up-regulation of immune response, including antigen presentation [*HLA-DPA1*, *HLA-DRA*, and *HLA-DQB1* (14, 15)], protection of T cells from cell death [*CD58* (16)], and T-cell activation [*FCER1A* (17, 18); Table 4]. In contrast, genes associated with progression were involved in immunosuppression [*CNR2* (19–21) and *NEATC4* (22, 23)], acute phase response and inflammation [*CRP* (24), *ORMS* (25, 26), *SERPINA7*, and *SERPINA1* (27, 28)], or a decrease in the level of B and T cells [*NFRKB* (23, 29)]. Three genes identified by the EASE program [*MBP* (30–32), *INHBB*, and *CMKLR1* (33, 34)] had unknown functions but are speculated to play a role in immune response. All 5 of the immune genes associated with regression and 2 (*CRP* and *MBP*) of the 10 immune genes associated with progression also had gene expression ranges that exceeded 2-fold.

Discussion

A separate analysis of the current microarray data examined the effect of treatment on gene expression without regard to final histology status and found that intervention with selenomethionine was not associated with alterations in gene expression in the normal mucosa of the esophagus (35). Because we did not observe a treatment effect on gene expression, we asked a second question

focused on the underlying cause of progression and regression in esophageal dysplasia. In the current analysis, we examined gene expression differences associated with morphologic changes over the 10-month intervention period to identify genes or groups of genes associated with the natural history of premalignant squamous esophageal lesions.

Immune response was the only pathway with more differentially expressed genes than expected based on the total number of such genes examined on the microarray. Among differentially expressed immune response genes, those associated with regression involved immune stimulation, whereas those associated with progression related to immune suppression and inflammation. Differences in the underlying immune response between these two groups may be important in distinguishing mechanisms associated with regression and progression of preneoplastic lesions. Immune reactions may be of critical importance in the enhancement or impairment of tumor oncogenic capacity. Human neoplastic cells express tumor-associated antigens in ways that immunologically differentiate them from normal, and the immune system may be activated to effectively react against these tumor cells (36). Genes associated with antigen presentation, similar to those observed in regression here, produce a cascade of events that leads to activation and expansion of T cells as well as the local accumulation of immune cells. These events may result in the elimination of cells, tissue repair, and resolution of inflammation. In contrast to this focal immune response, progression of preneoplastic lesions is believed, in part, to be caused by the subversion of immune response and the appearance of a more generalized inflammatory reaction (37–40). The most simplistic explanation for this phenotype is that defective antigen presentation in preneoplastic/tumor cells does not produce an adequate immune response (41).

Other groups of genes that were common in our 149 differentially expressed genes included genes related to the cell cycle ($n = 15$), metabolism ($n = 15$), and calcium transport or calcium ion activity ($n = 10$). Fifteen cell cycle-related genes were differentially expressed in this analysis, including 3 genes (*CDC14B*, *TGF- α* , and *RET*), whose range of gene expression was at least 2-fold. Fourteen of these cell cycle genes were overexpressed in individuals whose lesions progressed. Although the exact function of many of these genes is unknown, some have been shown to play an important role in the cell cycle and/or have been implicated in the progression of cancer. *TGF- α* , for example, is often overexpressed in head and neck and other squamous cell carcinomas and is believed to be a potent mitogen involved in wound healing (42). Its overexpression is thought to be an early event, found in both dysplasia and normal mucosa surrounding dysplastic tissue (43, 44). Two other potent mitogens, *MET* and *RET*, which are tyrosine kinase proto-oncogenes, are also involved in a variety of cancers (45, 46).

Fifteen genes involved in endogenous or xenobiotic metabolism were found to be significantly associated with change in worst squamous diagnosis. Several of the significantly associated genes (*AGPAT3*, *ATP5J*, and *ATP12A*) play a role in ATP metabolism, and increased expression was associated with progression, which suggests a response to increased energy requirements.

Genes involved in calcium regulation and calcium signaling also seemed to be important in the progression of esophageal squamous dysplasia. We found significant associations with 10 calcium-related genes. A recent array study that compared ESCC tumor and normal squamous tissue found a large number of changes in calcium-binding or calcium-modulating genes (47). One notable gene associated with progression of squamous dysplasia in

Table 3. One hundred twenty-nine genes whose increased expression was associated with progression of dysplasia

| Gene name or Affymetrix ID | Gene symbol | UniGene ID | β^* | Range of gene expression | P |
|---|------------------|------------|-----------|--------------------------|----------|
| Cytochrome P450, family 2, subfamily B, polypeptide 7 pseudogene 1 | <i>CYP2B7P1</i> | Hs.529117 | 1.191 | 3.78 | 0.000683 |
| EPH receptor B1 | <i>EPHB1</i> | Hs.116092 | 1.462 | 2.32 | 0.000807 |
| CDC14 cell division cycle 14 homologue B (S. cerevisiae) | <i>CDC14B</i> | Hs.40582 | 1.499 | 2.54 | 0.000919 |
| Myelin basic protein | <i>MBP</i> | Hs.501262 | 1.514 | 2.42 | 0.000466 |
| CDNA FLJ11433 fis, clone HEMBA1001121 | — | Hs.311790 | 1.529 | 2.50 | 0.000677 |
| Glutamate receptor, ionotropic, N-methyl D-aspartate 1 | <i>GRIN1</i> | Hs.495496 | 1.540 | 2.12 | 0.000892 |
| UDP glucuronosyltransferase 2 family, polypeptide B28 | <i>UGT2B28</i> | Hs.137585 | 1.634 | 2.23 | 0.000887 |
| Nuclear receptor subfamily 4, group A, member 3 | <i>NR4A3</i> | Hs.279522 | 1.646 | 2.54 | 0.000249 |
| MAS1 oncogene | <i>MAS1</i> | Hs.99900 | 1.696 | 2.33 | 0.000389 |
| Stanniocalcin 2 | <i>STC2</i> | Hs.233160 | 1.701 | 2.11 | 0.000620 |
| Solute carrier family 29 (nucleoside transporters), member 1 | <i>SLC29A1</i> | Hs.25450 | 1.702 | 1.90 | 0.000946 |
| Cell division cycle 25C | <i>CDC25C</i> | Hs.656 | 1.737 | 1.98 | 0.000683 |
| BCL2-associated X protein | <i>BAX</i> | Hs.159428 | 1.743 | 2.00 | 0.000951 |
| Sex determining region Y (SRY)-box 2 | <i>SOX2</i> | Hs.518438 | 1.744 | 2.27 | 0.000949 |
| Myosin phosphatase-Rho interacting protein | <i>M-RIP</i> | Hs.462341 | 1.748 | 2.27 | 0.000517 |
| CMT1A duplicated region transcript 1 | <i>CDRT1</i> | Hs.454698 | 1.783 | 2.02 | 0.000925 |
| Zona pellucida glycoprotein 2 (sperm receptor) | <i>ZP2</i> | Hs.73982 | 1.791 | 2.84 | 0.000167 |
| Dystonin | <i>DST</i> | Hs.485616 | 1.796 | 2.51 | 0.000906 |
| Postmeiotic segregation increased 2-like 11 | <i>PMS2L11</i> | — | 1.817 | 2.10 | 0.000299 |
| Early growth response 4 | <i>EGR4</i> | Hs.549031 | 1.832 | 1.86 | 0.000848 |
| Glycosyltransferase-like domain containing 1 | <i>GTDC1</i> | Hs.44780 | 1.871 | 2.25 | 0.000215 |
| Transforming growth factor, α | <i>TGFA</i> | Hs.170009 | 1.927 | 2.10 | 0.000192 |
| CDNA: FLJ22812 fis, clone KAIA2955 | — | Hs.540193 | 1.929 | 1.88 | 0.000220 |
| Cell death-inducing DFFA-like effector c | <i>CIDEA</i> | Hs.375023 | 1.943 | 1.98 | 0.000609 |
| 216732_at | — | — | 1.946 | 2.14 | 0.000981 |
| Basic leucine zipper nuclear factor 1 (JEM-1) | <i>BLZF1</i> | Hs.494326 | 1.957 | 2.14 | 0.000122 |
| Transmembrane and coiled-coil domains 2 | <i>TMCC2</i> | Hs.6360 | 1.960 | 2.06 | 0.000261 |
| Tudor domain containing 1 | <i>TDRD1</i> | Hs.333132 | 1.977 | 2.04 | 0.000694 |
| Myosin IB | <i>MYO1B</i> | Hs.439620 | 1.979 | 1.87 | 0.000062 |
| Hypothetical protein FLJ10770 | <i>KIAA1579</i> | Hs.207538 | 1.984 | 2.09 | 0.000832 |
| Receptor (calcitonin) activity modifying protein 3 | <i>RAMP3</i> | Hs.25691 | 2.000 | 1.89 | 0.000730 |
| Atrophin-1 interacting protein 1 | <i>AIP1</i> | Hs.488945 | 2.016 | 2.04 | 0.000117 |
| Tubulin, $\beta 4$ | <i>TUBB4</i> | Hs.110837 | 2.023 | 2.25 | 0.000069 |
| Dopachrome tautomerase | <i>DCT</i> | Hs.301865 | 2.055 | 1.94 | 0.000392 |
| ATPase, H ⁺ /K ⁺ transporting, nongastric, α polypeptide | <i>ATP12A</i> | Hs.147111 | 2.091 | 1.82 | 0.000997 |
| Natriuretic peptide precursor B | <i>NPPB</i> | Hs.219140 | 2.120 | 1.76 | 0.000988 |
| Ret proto-oncogene | <i>RET</i> | Hs.350321 | 2.128 | 2.21 | 0.000050 |
| Tenascin XB | <i>TNXB</i> | Hs.485104 | 2.136 | 1.80 | 0.000735 |
| Met proto-oncogene | <i>MET</i> | Hs.132966 | 2.176 | 1.70 | 0.000638 |
| Inhibin, β B (activin AB β polypeptide) | <i>INHBB</i> | Hs.1735 | 2.179 | 1.80 | 0.000747 |
| Fragile X mental retardation 2 | <i>FMR2</i> | Hs.496911 | 2.190 | 1.85 | 0.000082 |
| Serine (or cysteine) proteinase inhibitor, clade A member 7 | <i>SERPINA7</i> | Hs.76838 | 2.201 | 1.87 | 0.000167 |
| Adenylate cyclase 2 (brain) | <i>ADCY2</i> | Hs.481545 | 2.214 | 2.00 | 0.000095 |
| Solute carrier family 16 member 3 | <i>SLC16A3</i> | Hs.500761 | 2.226 | 2.04 | 0.000021 |
| Ca ²⁺ -dependent secretion activator | <i>CADPS</i> | Hs.127013 | 2.228 | 1.82 | 0.000695 |
| Zinc finger protein, subfamily 1A, 1 (Ikaro) | <i>ZNFN1A1</i> | Hs.435949 | 2.230 | 1.80 | 0.000952 |
| Interleukin (IL)-9 receptor | <i>IL9R</i> | Hs.549348 | 2.231 | 1.73 | 0.000888 |
| C-reactive protein, pentraxin related | <i>CRP</i> | Hs.76452 | 2.245 | 2.06 | 0.000959 |
| Zinc finger and BTB domain containing 7A | <i>ZBTB7A</i> | Hs.465623 | 2.246 | 2.03 | 0.000012 |
| Breast carcinoma amplified sequence 3 | <i>BCAS3</i> | Hs.463702 | 2.252 | 1.88 | 0.000006 |
| ATP synthase, H ⁺ transporting, mitochondrial F0 complex, subunit c (subunit 9), isoform 2 | <i>ATP5G2</i> | Hs.524464 | 2.275 | 1.71 | 0.000774 |
| 1-acylglycerol-3-phosphate O-acyltransferase 3 | <i>AGPAT3</i> | Hs.248785 | 2.331 | 1.65 | 0.000655 |
| Solute carrier family 22 member 1-like antisense | <i>SLC22A1LS</i> | Hs.300076 | 2.336 | 1.63 | 0.000653 |
| Transmembrane protease, serine 5 (spinesin) | <i>TMPRSS5</i> | Hs.46720 | 2.337 | 1.72 | 0.000180 |
| PR domain containing 10 | <i>PRDM10</i> | Hs.275086 | 2.348 | 1.72 | 0.000192 |

(Continued on the following page)

Table 3. One hundred twenty-nine genes whose increased expression was associated with progression of dysplasia (Cont'd)

| Gene name or Affymetrix ID | Gene symbol | UniGene ID | β^* | Range of gene expression | P |
|---|--------------------|------------|-----------|--------------------------|----------|
| Myotubularin-related protein 3 | <i>MTMR3</i> | Hs.474536 | 2.357 | 1.99 | 0.000373 |
| Ubiquitin-specific protease 7 | <i>USP7</i> | Hs.386939 | 2.363 | 1.86 | 0.000667 |
| Methylthioadenosine phosphorylase | <i>MTAP</i> | Hs.193268 | 2.380 | 1.72 | 0.000073 |
| Discs, large homologue 3 | <i>DLG3</i> | Hs.522680 | 2.381 | 1.79 | 0.000267 |
| Cadherin 9, type 2 | <i>CDH9</i> | Hs.272212 | 2.385 | 1.91 | 0.000220 |
| Uridine monophosphate synthetase | <i>UMPS</i> | Hs.2057 | 2.392 | 1.74 | 0.000254 |
| Orosomucoid 2 | <i>ORM2</i> | Hs.522356 | 2.433 | 1.66 | 0.000670 |
| Gem-associated protein 7 | <i>GEMIN7</i> | Hs.466919 | 2.457 | 1.65 | 0.000392 |
| 216812_at | — | — | 2.461 | 1.68 | 0.000082 |
| Hydroxysteroid (11- β) dehydrogenase 1 | <i>HSD11B1</i> | Hs.195040 | 2.464 | 1.70 | 0.000523 |
| Hypothetical gene supported by BC040718 | — | Hs.141055 | 2.466 | 1.72 | 0.000437 |
| Cytokine-induced protein 29 kDa | <i>CIP29</i> | Hs.505676 | 2.467 | 1.97 | 0.000085 |
| Transmembrane protein SHREW1 | <i>SHREW1</i> | Hs.25924 | 2.497 | 1.89 | 0.000320 |
| Rheumatoid arthritis synovium immunoglobulin heavy chain variable region | — | Hs.535413 | 2.497 | 1.70 | 0.000464 |
| Solute carrier family 10 member 2 | <i>SLC10A2</i> | Hs.194783 | 2.499 | 1.91 | 0.000427 |
| collagen, type I, α 1 | <i>COL1A1</i> | Hs.172928 | 2.511 | 1.64 | 0.000243 |
| Minor histocompatibility antigen HB-1 | <i>HB-1</i> | Hs.158320 | 2.520 | 1.88 | 0.000756 |
| Steroid-5- α -reductase, α polypeptide 2 | <i>SRD5A2</i> | Hs.458345 | 2.533 | 1.70 | 0.000742 |
| Hypothetical protein FLJ20184 | <i>FLJ20184</i> | Hs.272787 | 2.536 | 2.12 | 0.000040 |
| Cannabinoid receptor 2 | <i>CNR2</i> | Hs.73037 | 2.553 | 1.87 | 0.000170 |
| Chemokine-like receptor 1 | <i>CMKLR1</i> | Hs.506659 | 2.595 | 1.73 | 0.000160 |
| Amyloid β (A4) precursor protein-binding, family B, member 2 (Fe65-like) | <i>APBB2</i> | Hs.479602 | 2.595 | 1.70 | 0.000136 |
| Glycoprotein 2 | <i>GP2</i> | Hs.53985 | 2.601 | 1.68 | 0.000268 |
| G protein-coupled receptor 15 | <i>GPR15</i> | Hs.159900 | 2.601 | 1.54 | 0.000340 |
| Caspase-2, apoptosis-related cysteine protease | <i>CASP2</i> | Hs.368982 | 2.604 | 1.86 | 0.000076 |
| General transcription factor IIA, 1, 19/37 kDa | <i>GTF2A1</i> | Hs.510068 | 2.624 | 1.54 | 0.000532 |
| Nuclear factor of activated T-cells, cytoplasmic, calcineurin-dependent 4 | <i>NFATC4</i> | Hs.77810 | 2.637 | 1.60 | 0.000464 |
| Keratin, hair, basic, 5 | <i>KRTHB5</i> | Hs.182507 | 2.656 | 1.57 | 0.000577 |
| Transmembrane protein 24 | <i>TMEM24</i> | Hs.26899 | 2.681 | 1.72 | 0.000349 |
| Prepronociceptin | <i>PNOC</i> | Hs.88218 | 2.693 | 1.57 | 0.000939 |
| Peroxisome proliferative activated receptor, α | <i>PPARA</i> | Hs.275711 | 2.729 | 1.65 | 0.000182 |
| Glucosidase, β , acid 3 (cytosolic) | <i>GBA3</i> | Hs.371763 | 2.756 | 1.62 | 0.000385 |
| Pparl | — | Hs.272401 | 2.776 | 1.67 | 0.000651 |
| Nuclear factor related to κ B binding protein | <i>NFRKB</i> | Hs.530539 | 2.784 | 1.60 | 0.000044 |
| Apolipoprotein B mRNA editing enzyme, catalytic polypeptide-like 3G/3F | <i>APOBEC3G/3F</i> | Hs.474853 | 2.790 | 1.64 | 0.000468 |
| Keratin-associated protein 5-8 | <i>KRTAP5-8</i> | Hs.445245 | 2.797 | 1.51 | 0.000328 |
| RAS-like, family 11, member B | <i>RASL11B</i> | Hs.8035 | 2.805 | 1.53 | 0.000565 |
| Zinc finger, ZZ type with EF hand domain 1 | <i>ZZEF1</i> | Hs.277624 | 2.824 | 1.58 | 0.000756 |
| Zinc finger protein 42 (myeloid-specific retinoic acid-responsive) | <i>ZNF42</i> | Hs.399810 | 2.855 | 1.51 | 0.000157 |
| KIAA0953 | <i>KIAA0953</i> | Hs.227850 | 2.860 | 1.68 | 0.000093 |
| Serine (or cysteine) proteinase inhibitor, clade A (α -1 antitrypsin, antitrypsin), member 1 | <i>SERPINA1</i> | Hs.525557 | 2.863 | 1.67 | 0.000108 |
| Myosin binding protein C, cardiac | <i>MYBPC3</i> | Hs.524906 | 2.872 | 1.69 | 0.000010 |
| Astrotactin | <i>ASTN</i> | Hs.495897 | 2.875 | 1.64 | 0.000285 |
| GLIS family zinc finger 1 | <i>GLIS1</i> | Hs.306691 | 2.938 | 1.53 | 0.000094 |
| Solute carrier family 9 isoform 5 | <i>SLC9A5</i> | Hs.439650 | 2.953 | 1.44 | 0.000841 |
| 207748_at | <i>DARS</i> | — | 2.954 | 1.52 | 0.000759 |
| Suppressor of cytokine signaling 1 | <i>SOCS1</i> | Hs.50640 | 2.958 | 1.50 | 0.000475 |
| Testis expressed sequence 14 | <i>TEX14</i> | Hs.390221 | 2.976 | 1.75 | 0.000036 |
| Cancer/testis antigen 1B/1A | <i>CTAG1B/1A</i> | Hs.534310 | 2.990 | 1.56 | 0.000638 |
| PH domain and leucine-rich repeat protein phosphatase-like | <i>PHLPPL</i> | Hs.531564 | 2.990 | 1.71 | 0.000119 |
| Cell division cycle 42 (GTP binding protein, 25 kDa) | <i>CDC42</i> | Hs.467637 | 3.029 | 1.51 | 0.000230 |

(Continued on the following page)

Table 3. One hundred twenty-nine genes whose increased expression was associated with progression of dysplasia (Cont'd)

| Gene name or Affymetrix ID | Gene symbol | UniGene ID | β^* | Range of gene expression | P |
|--|------------------|------------|-----------|--------------------------|----------|
| Choline acetyltransferase | <i>CHAT</i> | Hs.302002 | 3.042 | 1.67 | 0.000049 |
| Glycoprotein VI (platelet) | <i>GP6</i> | Hs.272216 | 3.103 | 1.55 | 0.000924 |
| ATP-binding cassette, subfamily A (ABC1), member 1 | <i>ABCA1</i> | Hs.429294 | 3.133 | 1.54 | 0.000663 |
| MRNA; cDNA DKFZp434M0835 | — | Hs.406781 | 3.254 | 1.49 | 0.000966 |
| Kinase D-interacting substance of 220 kDa | <i>KIDINS220</i> | Hs.9873 | 3.365 | 1.51 | 0.000739 |
| Sema domain, immunoglobulin domain (Ig), transmembrane domain (TM) and short cytoplasmic domain, (semaphorin) 4F | <i>SEMA4F</i> | Hs.25887 | 3.381 | 1.65 | 0.000092 |
| Phosphate regulating endopeptidase homologue, X-linked | <i>PHEX</i> | Hs.495834 | 3.389 | 1.40 | 0.000711 |
| Thioredoxin reductase 2 | <i>TXNRD2</i> | Hs.443430 | 3.425 | 1.58 | 0.000090 |
| Thrombospondin 1 | <i>THBS1</i> | Hs.164226 | 3.453 | 1.41 | 0.000839 |
| BRCA1-associated protein | <i>BRAP</i> | Hs.530940 | 3.489 | 1.42 | 0.000342 |
| Similar to supervillin isoform 2 | <i>LOC387648</i> | Hs.408581 | 3.607 | 1.40 | 0.000893 |
| SNF1-like kinase 2 | <i>SNF1LK2</i> | Hs.552588 | 3.668 | 1.47 | 0.000269 |
| KIAA0194 protein | <i>KIAA0194</i> | Hs.549664 | 3.686 | 1.39 | 0.000219 |
| Transient receptor potential cation channel, subfamily C, member 4 | <i>TRPC4</i> | Hs.262960 | 3.703 | 1.47 | 0.000549 |
| Brain-specific angiogenesis inhibitor 3 | <i>BAI3</i> | Hs.13261 | 3.895 | 1.46 | 0.000226 |
| Coagulation factor II (thrombin) receptor-like 2 | <i>F2RL2</i> | Hs.42502 | 3.955 | 1.38 | 0.000730 |
| 204898_at | <i>SAP30*</i> | — | 4.085 | 1.41 | 0.000625 |
| Tumor-associated calcium signal transducer 2 | <i>TACSTD2</i> | Hs.23582 | 4.131 | 1.43 | 0.000098 |
| Radixin | <i>RDX</i> | Hs.263671 | 4.137 | 1.29 | 0.000968 |
| Zinc finger protein 480 | <i>ZNF480</i> | Hs.147025 | 4.173 | 1.43 | 0.000456 |
| Pancreatic lipase-related protein 2 | <i>PNLIPRP2</i> | Hs.423598 | 4.546 | 1.40 | 0.000035 |
| T cell receptor α chain | <i>TRA</i> | Hs.546379 | 4.728 | 1.33 | 0.000620 |
| Tripartite motif-containing 10 | <i>TRIM10</i> | Hs.274295 | 5.324 | 1.26 | 0.000485 |

* β s were generated from the ordinal regression model, which defined regress as (−1), stable as (0), and progress as (1). One hundred twenty-nine genes were associated with progression. The more positive the value, the greater the association with progression.

our study is *tumor-associated calcium signal transducer 2* (*TACSTD2*; also known as *TROP-2*), which has previously been identified as a tumor antigen (48) that transduces calcium signals (49). The *TROP-2* protein has been reported to be overexpressed in the sera of

ESCC patients (50). The increased expression of this gene in the normal tissue of subjects without frank tumors suggests that this gene and protein may be important at an early stage of tumor formation.

Table 4. Fifteen genes in the immune response pathway associated with regression or progression

| Gene name | Gene function |
|---|---|
| Genes with higher expression in regression | |
| <i>FCER1A</i> | α Subunit of IgE high-affinity Fc receptor located on mast cells; expression results in the release of T-cell mediators that initiate an inflammatory response |
| <i>CD58</i> | Modulates cell adhesion and T-cell activation; may protect T cells from cell death |
| <i>HLA-DPA1</i> | Antigen presentation |
| <i>HLA-DRA</i> | Antigen presentation |
| <i>HLA-DQB1</i> | Antigen presentation |
| Genes with higher expression in progression | |
| <i>CRP</i> | Acute phase response; nonspecific marker for inflammation, positively correlated with cancer |
| <i>ORMS</i> | Acute phase response; protects tumors against immune mechanism |
| <i>SERPINA7</i> | Acute phase response; plays a role in inflammation, tumor invasion, apoptosis, fibrinolysis, and coagulation |
| <i>SERPINA1</i> | Acute phase response |
| <i>CNR2</i> | Immunosuppressive action, including inhibition of IL-2; may modulate NF-AT |
| <i>NFATC4</i> | Inflammatory response; decreases IL-2 transcription |
| <i>NFRKB</i> | Inflammatory response; decreases levels of B and/or T cells |
| <i>MBP</i> | Involved in immune response in multiple sclerosis; increased in cancer patients |
| <i>INHBB</i> | Cytokine activity |
| <i>CMKLR1</i> | Attracts macrophages and immature dendritic cells to inflammation; early response |

The results reported here represent a unique effort in carcinogenesis research to bridge the gap in our understanding between morphology and molecular biology. A cancer prevention trial was used, in which the primary end point, regression, or progression of a surrogate cancer end point (intraepithelial neoplasia) was evaluated in relation to change in gene expression profiles from the beginning to the end of the intervention (51). Because the trial found that supplementation with selenium improved the morphologic profile among participants who started the trial with mild dysplasia, we were able to examine molecular changes (changes in RNA expression profiles) coincidental with morphologic changes. All the genes identified here are of interest because of their potential role in the natural history of esophageal squamous dysplasia. In addition, as part of future cancer prevention strategies, the genes associated with regression represent potential targets for gene or pathway enhancement and the genes associated with progression are potential targets for pathway disruption. Similarly, both regression- and progression-associated genes merit consideration as early detection markers.

There are several caveats that should be considered in evaluating this study. The tissues analyzed here were only from histologically normal esophageal tissue in persons with dysplasia elsewhere in

their esophagus. We do not know if gene expression results would be the same if the premalignant lesions themselves had been analyzed. Although there were several strong design features built into this study (i.e., the end point was the paired before-versus-after supplementation morphology difference in a single individual, and the exposure was the paired before-versus-after supplementation gene expression profile in the same person), the study was only modest in size. It should thus be considered an exploratory effort for which the findings must be replicated elsewhere using different study populations and alternative study designs.

In conclusion, we examined the association between gene expression changes over a 10-month period in normal esophageal mucosal biopsy specimens and regression, stability, and progression in worst esophageal squamous lesions. We found many significant associations, including numerous genes involved in immune response.

Acknowledgments

Received 2/20/2006; revised 4/25/2006; accepted 5/4/2006.

The costs of publication of this article were defrayed in part by the payment of page charges. This article must therefore be hereby marked *advertisement* in accordance with 18 U.S.C. Section 1734 solely to indicate this fact.

References

- Parkin DM, Bray F, Ferlay J, Pisani P. Global cancer statistics, 2002. *CA Cancer J Clin* 2005;55:74–108.
- Brown LM, Devesa SS. Epidemiologic trends in esophageal and gastric cancer in the United States. *Surg Oncol Clin N Am* 2002;11:235–56.
- Wang GQ, Abnet CC, Shen Q, et al. Histological precursors of oesophageal squamous cell carcinoma: results from a 13 year prospective follow up study in a high risk population. *Gut* 2005;54:187–92.
- Mark SD, Qiao YL, Dawsey SM, et al. Prospective study of serum selenium levels and incident esophageal and gastric cancers. *J Natl Cancer Inst* 2000;92:1753–63.
- Funkhouser EM, Sharp GB. Aspirin and reduced risk of esophageal carcinoma. *Cancer* 1995;76:1116–9.
- Farrow DC, Vaughan TL, Hansten PD, et al. Use of aspirin and other nonsteroidal anti-inflammatory drugs and risk of esophageal and gastric cancer. *Cancer Epidemiol Biomarkers Prev* 1998;7:97–102.
- Limburg PJ, Wei W, Ahnen DJ, et al. Randomized, placebo-controlled, esophageal squamous cell cancer chemoprevention trial of selenomethionine and celecoxib. *Gastroenterology* 2005;129:863–73.
- Dawsey SM, Lewin KJ, Liu FS, Wang GQ, Shen Q. Esophageal morphology from Linxian, China. Squamous histologic findings in 754 patients. *Cancer* 1994; 73:2027–37.
- Dawsey SM, Fleischer DE, Wang GQ, et al. Mucosal iodine staining improves endoscopic visualization of squamous dysplasia and squamous cell carcinoma of the esophagus in Linxian, China. *Cancer* 1998;83:220–31.
- Affymetrix. GeneChip expression analysis technical manual. Santa Clara (CA): Affymetrix; 2001.
- Dennis G, Jr., Sherman BT, Hosack DA, et al. DAVID: database for annotation, visualization, and integrated discovery. *Genome Biol* 2003;4:3.
- Bender R, Ulrich G. Ordinal logistic regression in medical research. *J R Coll Physicians Lond* 1997;31: 546–51.
- Hosack DA, Dennis G, Jr., Sherman BT, Lane HC, Lempicki RA. Identifying biological themes within lists of genes with EASE. *Genome Biol* 2003;4:R70.
- Lantermann A, Hampe J, Kim WH, et al. Investigation of HLA-DPA1 genotypes as predictors of inflammatory bowel disease in the German, South African, and South Korean populations. *Int J Colorectal Dis* 2002;17:238–44.
- Jordanova ES, Philippo K, Giphart MJ, Schuurin E, Kluijn PM. Mutations in the HLA class II genes leading to loss of expression of HLA-DR and HLA-DQ in diffuse large B-cell lymphoma. *Immunogenetics* 2003;55:203–9.
- Daniel PT, Scholz C, Essmann F, Westermann J, Pezzutto A, Dorken B. CD95/Fas-triggered apoptosis of activated T lymphocytes is prevented by dendritic cells through a CD58-dependent mechanism. *Exp Hematol* 1999;27:1402–8.
- Inomata N, Tomita H, Ikezawa Z, Saito H. Differential gene expression profile between cord blood progenitor-derived and adult progenitor-derived human mast cells. *Immunol Lett* 2005;98:265–71.
- Le Coniat M, Kinet JP, Berger R. The human genes for the α and γ subunits of the mast cell receptor for immunoglobulin E are located on human chromosome band 1q23. *Immunogenetics* 1990;32:183–6.
- Germain N, Boichot E, Advenier C, Berdyshev EV, Lagente V. Effect of the cannabinoid receptor ligand, WIN 55,212-2, on superoxide anion and TNF- α production by human mononuclear cells. *Int Immunopharmacol* 2002;2:537–43.
- Kaplan BL, Rockwell CE, Kaminski NE. Evidence for cannabinoid receptor-dependent and -independent mechanisms of action in leukocytes. *J Pharmacol Exp Ther* 2003;306:1077–85.
- Stapleton SR, Garlock GL, Foellmi-Adams L, Kletzien RF. Selenium: potent stimulator of tyrosyl phosphorylation and activator of MAP kinase. *Biochim Biophys Acta* 1997;1355:259–69.
- Jauliac S, Lopez-Rodriguez C, Shaw LM, Brown LF, Rao A, Toker A. The role of NFAT transcription factors in integrin-mediated carcinoma invasion. *Nat Cell Biol* 2002;4:540–4.
- Serfling E, Berberich-Siebelt F, Avots A, et al. NFAT and NF- κ B factors—the distant relatives. *Int J Biochem Cell Biol* 2004;36:1166–70.
- Mahmoud FA, Rivera NI. The role of C-reactive protein as a prognostic indicator in advanced cancer. *Curr Oncol Rep* 2002;4:250–5.
- Fan C, Stendahl U, Stjernberg N, Beckman L. Association between orosomucoid types and cancer. *Oncology* 1995;52:498–500.
- Tesarova P, Kvasnicka J, Umlaufova A, Homolkova J, Kalousova M, Tesar V. [Acute phase proteins in female patients with breast carcinoma]. *Sb Lek* 2003;104:121–32.
- Kummer JA, Strik MC, Bladergroen BA, Hack CE. Production, characterization, and use of serpin antibodies. *Methods* 2004;32:141–9.
- Morgan K, Kalsheker NA. Regulation of the serine proteinase inhibitor (SERPIN) gene α 1-antitrypsin: a paradigm for other SERPINs. *Int J Biochem Cell Biol* 1997;29:1501–11.
- Ounap K, Bartsch O, Uibo O, Laidre P. Girl with combined cellular immunodeficiency, pancytopenia, malformations, deletion 11q23.3 \rightarrow qter, and trisomy 8q24.3 \rightarrow qter. *Am J Med Genet* 2002;108:322–6.
- Gouda Z, Thomson DM. Measurement by leukocyte adherence inhibition of autosensitization of cancer patients to myelin basic protein. *Jpn J Cancer Res* 1988;79:529–37.
- Puri J, Arnon R, Gurevich E, Teitelbaum D. Modulation of the immune response in multiple sclerosis: production of monoclonal antibodies specific to HLA/myelin basic protein. *J Immunol* 1997;158:2471–6.
- Usuku K. [Immune response against myelin basic protein and analysis of T-cell receptor in multiple sclerosis]. *Nippon Rinsho* 1994;52:2932–9.
- Meder W, Wendland M, Busmann A, et al. Characterization of human circulating TIG2 as a ligand for the orphan receptor ChemR23. *FEBS Lett* 2003;555:495–9.
- Wittamer V, Franssen JD, Vulcano M, et al. Specific recruitment of antigen-presenting cells by chemerin, a novel processed ligand from human inflammatory fluids. *J Exp Med* 2003;198:977–85.
- Joshi N, Johnson LL, Wei WQ, et al. Selenomethionine treatment does not alter gene expression in normal squamous esophageal mucosa in a high-risk Chinese population. *Cancer Epidemiol Biomarkers Prev* 2006;15: 1–3.
- Spadaro M, Lanzardo S, Curcio C, Forni G, Cavallo F. Immunological inhibition of carcinogenesis. *Cancer Immunol Immunother* 2004;53:204–16.
- Emens LA, Jaffee EM. Cancer vaccines: an old idea comes of age. *Cancer Biol Ther* 2003;2:S161–8.
- Finn OJ. Cancer vaccines: between the idea and the reality. *Nat Rev Immunol* 2003;3:630–41.
- Matzinger P. The danger model: a renewed sense of self. *Science* 2002;296:301–5.
- Pardoll D. Does the immune system see tumors as foreign or self? *Annu Rev Immunol* 2003;21:807–39.
- Jakobisiak M, Lasek W, Golab J. Natural mechanisms protecting against cancer. *Immunol Lett* 2003;90:103–22.
- Bridges AJ. The rationale and strategy used to develop a series of highly potent, irreversible, inhibitors of the epidermal growth factor receptor family of tyrosine kinases. *Curr Med Chem* 1999;6:825–43.

43. Srinivasan M, Jewell SD. Evaluation of TGF- α and EGFR expression in oral leukoplakia and oral submucous fibrosis by quantitative immunohistochemistry. *Oncology* 2001;61:284–92.
44. Yang B, Li F. Quantitative analysis of TGF- α and EGFR mRNA in laryngeal carcinoma tissues. *Chin Med J (Engl)* 1999;112:1088–92.
45. Carlomagno F, Santoro M. Receptor tyrosine kinases as targets for anticancer therapeutics. *Curr Med Chem* 2005;12:1773–81.
46. Longati P, Comoglio PM, Bardelli A. Receptor tyrosine kinases as therapeutic targets: the model of the MET oncogene. *Curr Drug Targets* 2001;2:41–55.
47. Luo A, Kong J, Hu G, et al. Discovery of Ca²⁺-relevant and differentiation-associated genes downregulated in esophageal squamous cell carcinoma using cDNA microarray. *Oncogene* 2004;23:1291–9.
48. Fornaro M, Dell'Arciprete R, Stella M, et al. Cloning of the gene encoding Trop-2, a cell-surface glycoprotein expressed by human carcinomas. *Int J Cancer* 1995;62: 610–8.
49. Ripani E, Sacchetti A, Corda D, Alberti S. Human Trop-2 is a tumor-associated calcium signal transducer. *Int J Cancer* 1998;76:671–6.
50. Nakashima K, Shimada H, Ochiai T, et al. Serological identification of TROP2 by recombinant cDNA expression cloning using sera of patients with esophageal squamous cell carcinoma. *Int J Cancer* 2004;112:1029–35.
51. O'Shaughnessy JA, Kelloff GJ, Gordon GB, et al. Treatment and prevention of intraepithelial neoplasia: an important target for accelerated new agent development. *Clin Cancer Res* 2002;8:314–46.